

---

# Boosting Generalization Performance in Model-Heterogeneous Federated Learning Using Variational Transposed Convolution

---

**Ziru Niu**  
RMIT University  
Melbourne, VIC, Australia  
ziru.niu@student.rmit.edu.au

**Hai Dong\***  
RMIT University  
Melbourne, VIC, Australia  
hai.dong@rmit.edu.au

**A. K. Qin**  
Swinburne University of Technology  
Hawthorn, VIC, Australia  
kqin@swin.edu.au

## Abstract

Federated learning (FL) is a pioneering machine learning paradigm that enables distributed clients to process local data effectively while ensuring data privacy. However, the efficacy of FL is usually impeded by the data heterogeneity among clients, resulting in local models with low generalization performance. To address this problem, traditional model-homogeneous approaches mainly involve debiasing the local training procedures with regularization or dynamically adjusting client weights in aggregation. Nonetheless, these approaches become incompatible for scenarios where clients exhibit heterogeneous model architectures. In this paper, we propose a model-heterogeneous FL framework that can improve clients' generalization performance over unseen data without model aggregation. Instead of model parameters, clients exchange the feature distributions with the server, including the mean and the covariance. Accordingly, clients train a variational transposed convolutional (VTC) neural network with Gaussian latent variables sampled from the feature distributions, and use the VTC model to generate synthetic data. By fine-tuning local models with the synthetic data, clients significantly increase their generalization performance. Experimental results show that our approach obtains higher generalization accuracy than existing model-heterogeneous FL frameworks, as well as lower communication costs and memory consumption.

## 1 Introduction

The prevalence of the Internet of Things (IoT) propels federated learning (FL) [1] as a widespread technique to process the dispersed data among end clients while ensuring data privacy. Under the regulation of a central server, clients collaboratively train a global model without revealing any personal data, and exchange the model parameters with the server. Abstaining from data transmission, FL markedly alleviates communication overhead and the risk of data leakage. However, the inherent data heterogeneity of IoT clients presents significant challenges to FL. Firstly, clients comprise edge devices distributed across various geographical locations, which naturally collect non-identically-independent data [2]. Secondly, single clients usually collect real-time data with frequent distribution shifts in practical scenarios, such as weather forecasting [3, 4] and healthcare [5].

---

\*Corresponding author.

To overcome both inter-client and intra-client data heterogeneities, improving the *generalization* ability (i.e., the ability to predict unseen data correctly [6]) of clients has become a vital matter in FL [7]. Existing solutions mainly focus on two aspects, including regularization and weight modification. Regularization methods propose to debias the individual training process by imposing a regularization term on the local objective function of clients [8, 9, 10, 11, 12, 13, 14, 15]. Weight modification methods aim to alleviate the negative impact of biased clients on the global model, including assigning lower weights to biased entities in aggregation [16, 17, 18, 19, 20] or reducing the possibility of selecting these clients [21, 22, 23, 24, 25]. As a result, the global model maintains significant robustness against the heterogeneous client data. Correspondingly, clients can improve their generalization performance by incorporating the enhanced global model into their local models.

Despite the outstanding progress in addressing data heterogeneity, the aforementioned works are developed based on the assumption that all clients share the same model architecture. In practice, clients are likely to obtain personalized models with diverse and irrelevant architectures [7], referred to as *model-heterogeneous* FL (see Appendix A for details), making traditional aggregation-based methods prohibitive. In this case, clients cannot learn generalized information through parameter sharing, which necessitates alternative strategies for enhancing the generalization of local models with differing architectures.

Several attempts have been made to improve the generalization of model-heterogeneous FL through knowledge distillation [26, 27, 28, 29, 30, 31, 32]. These works utilize a shared public dataset and enable clients to exchange knowledge by comparing each other’s predictions on the dataset. However, the prerequisite of a **public dataset** severely restricts the deployment of these works, as a public dataset is usually not available in real-world circumstances [33].

To address this concern, data-free model-heterogeneous FL methods have been proposed, which can mainly be divided into two categories. The first category employs generated feature representations for knowledge distillation [33, 34], eliminating the dependence on public datasets. However, unlike raw samples, knowledge distillation on feature space merely regularizes the head classifier of a local model, while leaving the backbone feature extractor unmodified. The second category involves circumventing knowledge distillation and enabling clients to communicate through alternative messages, such as mean feature representations [35, 36] and a mutual proxy model [37]. Although [35, 36] regularizes local feature extractors by enforcing them to derive unbiased feature representations, the biased head classifiers are neglected in these works, which significantly limits the generalization improvement. For [37], training and transmitting an overparameterized proxy model [37] will result in substantial communication and memory overhead.

To overcome the disadvantages of prior methods, we expect a comprehensive FL framework that can increase the generalization of model-heterogeneous clients without relying on any public dataset, while maintaining communication and memory efficiency. To this end, we propose **FedVTC** (Federated Learning with Variational Transposed Convolution), a model-heterogeneous FL framework that uses synthetic data to fine-tune local models, thus improving generalization without relying on a public dataset. FedVTC achieves this by enabling each client to generate synthetic samples using a variational transposed convolutional (VTC) neural network. The VTC model takes low-dimensional Gaussian latent variables as input and produces corresponding synthetic samples by upsampling the latent variables. Afterwards, clients fine-tune the local models with the synthetic samples to improve the generalization ability. In communication, clients only exchange the local mean and covariance with the server to mitigate the bias of local feature distributions, leading to substantial communication cost reduction. Compared with representation-based knowledge distillation [33, 34] that only regularizes the head classifier, fine-tuning with synthetic images can debias both the feature extractor and the classifier in a local model, thereby potentially achieving higher generalization performance. In addition, FedVTC enables clients to train the VTC model and local models alternately to avoid extra memory consumption.

Similar to a variational autoencoder (VAE), a VTC model is initially trained by maximizing the evidence lower bound (ELBO) of local data [38]. Moreover, to strengthen the robustness of VTC against variant input latent variables, we incorporate a Distribution Matching (DM) loss [39] into the objective function of VTC for regularization. This strategy helps FedVTC produce synthetic samples with better training quality, which notably improves the performance of the fine-tuned local models. The contributions of this paper are summarized as follows:

- We propose FedVTC, a model-heterogeneous FL framework based on variational transposed convolution. FedVTC uses synthetic data to fine-tune local models for better generalization, eradicating the dependence on pre-existing public datasets.
- We design a novel objective function to train the VTC model, which encompasses the standard negative ELBO loss and a DM loss. The DM loss regularizes the training procedure of VTC, enabling VTC to consistently generate high-quality synthetic samples with varying input latent variables.
- We conduct extensive experiments to validate the effectiveness of FedVTC. Experiment results show that FedVTC obtains higher generalization accuracy than existing model-heterogeneous FL frameworks over MNIST, CIFAR10, CIFAR100 and Tiny-ImageNet datasets, as well as lower or equivalent communication costs and memory consumption.

## 2 Literature Review

### 2.1 Improving the Generalization of Model-homogeneous Federated Learning

The endeavors of the state-of-the-art to enhance the generalization of model-homogeneous FL can mainly be divided into two categories, which are regularization and weight modification. **Regularization** approaches aim to debias the local training procedure by adding a regularization term onto the clients' local objective functions. For instance, [8, 9, 10, 12, 13, 14] prevent client models from overfitting to local optima by restricting the Euclidean distance between local and global parameters. Besides, [11] employs a relationship matrix to enforce clients with higher similarities to learn close parameter updates, and [15] alleviates the bias of local training using ridge regression.

**Weight modification** methods enhance the generalization of the global model by deducting the proportion of biased clients participating in global training. Subsequently, clients can also reinforce the generalization ability by incorporating the well-generalized global model into their local models. On one hand, [16, 17, 18, 19, 20] replace weighted average with dynamic weighting strategies, and assign lower weights to biased, anomalous and malicious parameter updates in aggregation. On the other hand, [21, 22, 23, 24, 25] design some heuristic functions to evaluate the importance of each client, such as training loss and cosine similarity. Consequently, these works develop a selective client sampling strategy that selects unimportant entities with lower possibilities to mitigate the negative effect of biased clients.

Although these works have achieved remarkable progress in improving FL generalization, they are developed based on the assumption that all clients share a universal model architecture. For model-heterogeneous FL, where clients exhibit diverse model architectures, the aforementioned works become infeasible.

### 2.2 Model-heterogeneous Federated Learning

The most commonly used approach to improve the generalization of model-heterogeneous FL is **knowledge distillation** [26, 27, 28, 29, 30, 31, 32]. With the presence of a public dataset, clients are able to acquire unbiased global knowledge by learning from each other's predictions on the dataset. However, the prerequisite of a public dataset can be a critical bottleneck for these methods, as such a dataset is not usually available in practice.

To overcome the dependence on a public dataset, [33, 34] propose to use generative models, such as a generative adversarial network (GAN) and a multivariate Gaussian sampler, to generate feature representations for knowledge distillation. However, unlike raw samples that progress through all layers, feature representations merely go through the head classifier of a neural network. Consequently, the distillation scheme in [33, 34] only debiases the classifier of local models, which significantly limits the generalization improvement. Additionally, instead of knowledge distillation, [35, 36, 37] allows clients to exchange model-architecture-independent messages for generalization, such as the mean of feature representations [35, 37] and a common proxy model [37]. For one thing, representation sharing [35, 37] regularizes the backbone feature extractors in local models by enforcing clients to derive unbiased feature representations, while neglecting the head classifiers. For another thing, training and transmitting a proxy model [37] might cause undesired communication and memory costs.

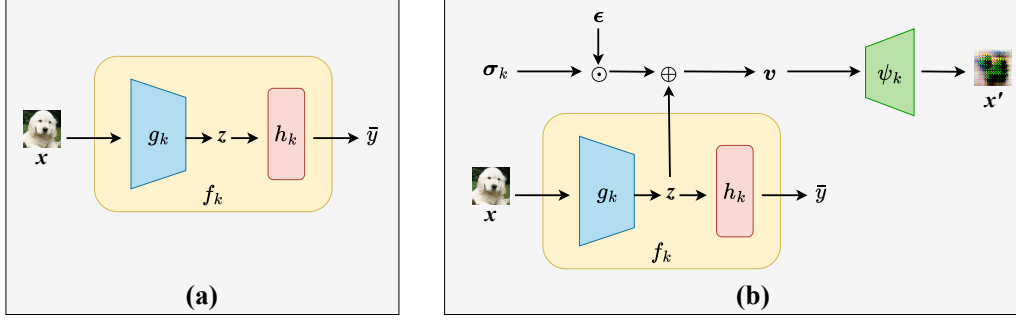


Figure 1: A comparison between: (a): a standard FL client and (b): a client in FedVTC. In (b), " $\oplus$ " and " $\odot$ " respectively standard for element-wise addition and product.

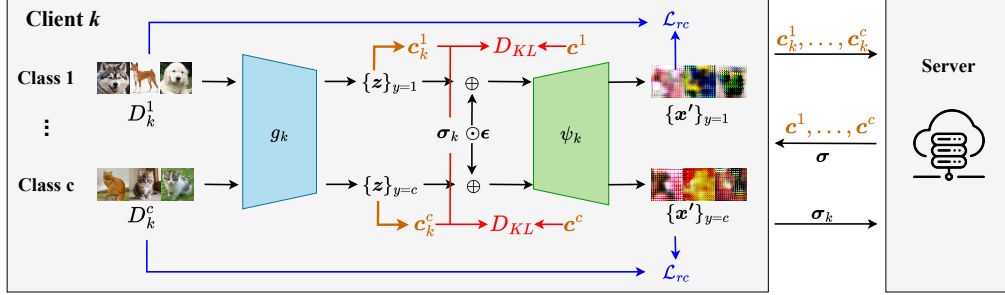


Figure 2: VTC is trained with loss function  $\mathcal{L}_e = \mathcal{L}_{rc} + D_{KL}$ .  $\mathcal{L}_{rc}$  (blue) is the reconstruction loss between the original samples and the generated samples, and  $D_{KL}$  (red) is the KL-divergence between the distributions of the local and global latent variables.

### 3 Methodology

#### 3.1 Preliminaries

Suppose a network consisting of a central server and a set of clients  $\mathcal{K} = \{1, 2, \dots, K\}$  with non-iid local datasets  $\{D_1, \dots, D_K\}$ . Each client  $k$  ( $1 \leq k \leq K$ ) obtains a local model  $f_k : \mathbb{R}^d \rightarrow \mathbb{R}$ , which can be decomposed into a backbone feature extractor  $g_k : \mathbb{R}^d \rightarrow \mathbb{R}^p$  and a head classifier  $h_k : \mathbb{R}^p \rightarrow \mathbb{R}$ . In formula,  $f_k = h_k \circ g_k$ . Let  $\{(x_i, y_i)\}_{1 \leq i \leq n_k}$  denote the collection of data in the local dataset  $D_k$  with a total of  $n_k = |D_k|$  samples. As shown in Figure 1(a), for each sample  $x \in \mathbb{R}^d$  with the corresponding label  $y \in \{1, 2, \dots, C\}$ ,  $f_k$  takes  $x$  as input and makes a prediction  $\bar{y}$ , where  $C$  is the total number of all possible classes. Firstly,  $x$  is transformed to a latent variable  $z \in \mathbb{R}^p$  using the feature extractor  $g_k$  (i.e.,  $z = g_k(x)$ ). Secondly,  $z$  is forwarded to the classifier  $h_k$  to produce a prediction  $\bar{y} = h_k(z)$ .

The objective of model-heterogeneous FL is to find the optimal set of local models  $\{f_1^*, \dots, f_K^*\}$  minimizing the local empirical loss, that is:

$$f_1^*, \dots, f_K^* = \arg \min_{f_1, \dots, f_K} \frac{1}{K} \sum_{k=1}^K \frac{1}{|D_k|} \sum_{(x,y) \in D_k} \mathcal{L}(y, f_k(x)) \quad (1)$$

$\mathcal{L}(y, f_k(x))$  is the classification loss (e.g. cross-entropy) of model  $f_k$  on the sample  $(x, y)$ . In addition, to evaluate generalization performance, we run each  $f_k$  on  $D_0$ , which is a test dataset consisting of unseen samples [6], that is,  $\forall k, D_0 \cap D_k = \emptyset$ .

#### 3.2 Variational Transposed Convolution

As Figure 1(b) shows, aside from the fundamental local model  $f_k$ , FedVTC introduces a variational transposed convolution (VTC) model  $\psi_k : \mathbb{R}^p \rightarrow \mathbb{R}^d$  to each client  $k$ . VTC is an upsampling network that takes a latent variable  $z \in \mathbb{R}^p$  as input to produce an enlarged data sample  $x' \in \mathbb{R}^d$  [40]. Similar

to a VAE [38], for each sample  $\mathbf{x}$  with the corresponding  $\mathbf{z}$ , client  $k$  samples a random variable  $\mathbf{v}$  from the distribution  $\mathcal{N}(\mathbf{v}|\mathbf{z}, \Sigma_k)$ , and forwards  $\mathbf{v}$  to  $\psi_k$  to derive  $\mathbf{x}'$ , the covariance matrix  $\Sigma_k \in \mathbb{R}^{p \times p}$  can be learned via the gradient method. To make  $\Sigma_k$  differentiable, FedVTC applies the well-known reparametrization trick as per VAE and lets  $\mathbf{v} = \mathbf{z} + \boldsymbol{\sigma}_k \odot \boldsymbol{\epsilon}$ .  $\boldsymbol{\epsilon} \in \mathbb{R}^p$  is a random Gaussian noise with distribution  $\boldsymbol{\epsilon} \sim \mathcal{N}(\boldsymbol{\epsilon}|\mathbf{0}, \mathbf{I})$ ,  $\boldsymbol{\sigma}_k = [\sigma_1, \sigma_2, \dots, \sigma_p]^\top$  indicates the reparameterized standard deviation (SD), and " $\odot$ " represents element-wise product. In this case, for each entry in  $\Sigma_k$ , we have  $(\Sigma_k)_{ii} = \sigma_i^2$  and  $(\Sigma_k)_{ij} = 0$  for any  $i \neq j$ , and each  $\sigma_i$  ( $1 \leq i \leq p$ ) can be learned through gradient descent.

Following the design of VAE [38], VTC is trained by maximizing the **evidence lower bound (ELBO)**, which is calculated as:

$$\text{ELBO} = \log p_{\psi_k}(\mathbf{x}'|\mathbf{z}, \boldsymbol{\sigma}_k) - D_{KL}(q_{g_k}(\mathbf{z}|\mathbf{x})||p(\mathbf{z})) \quad (2)$$

For each sample  $(\mathbf{x}, y)$  with latent variable  $\mathbf{z}$ , the log-likelihood  $\log p_{\psi_k}(\mathbf{x}'|\mathbf{z}, \boldsymbol{\sigma}_k)$  represents how  $\psi_k$  can generate real-world samples based on the latent variable  $\mathbf{z} + \boldsymbol{\sigma}_k \odot \boldsymbol{\epsilon}$ . According to [38], this term can be well approximated by minimizing the empirical reconstruction loss  $\mathcal{L}_{rc}(\mathbf{x}', \mathbf{x}) = \|\mathbf{x}' - \mathbf{x}\|_2^2$  as Figure 2 shows. The negative Kullback–Leibler (KL)-divergence  $-D_{KL}(q_{g_k}(\mathbf{z}|\mathbf{x})||p(\mathbf{z}))$  measures how  $q_{g_k}(\mathbf{z}|\mathbf{x})$  (the distribution of  $\mathbf{z}$  learned by the feature extractor  $g_k$ ) approaches the real distribution  $p(\mathbf{z})$ . Following [38], we can assume  $p(\mathbf{z}) \sim \mathcal{N}(\boldsymbol{\mu}, \mathbf{I})$ , with  $\boldsymbol{\mu}$  denoting the unbiased mean of  $\mathbf{z}$  which is usually  $\mathbf{0}$  by default. In FL settings, we follow [35] and estimate  $\boldsymbol{\mu}$  using  $\mathbf{c}^y$ , which is the global **prototype** of class  $y$ . As Figure 2 shows, a global prototype  $\mathbf{c}^y = \frac{1}{|\mathcal{K}_y|} \sum_{k \in \mathcal{K}_y} \mathbf{c}_k^y$  is calculated as the expectation of all local prototype  $\mathbf{c}_k^y$  for all  $k \in \mathcal{K}_y$ , with  $\mathcal{K}_y \subset \mathcal{K}$  indicating the set of all clients containing data of class  $y$ . A local prototype of client  $k$  is the mean of the local feature representations, i.e.  $\mathbf{c}_k^y = \frac{1}{|D_k^y|} \sum_{(\mathbf{x}, y) \in D_k^y} g_k(\mathbf{x})$ , where  $D_k^y \subset D_k$  indicates the collection of all samples of class  $y$  in local dataset  $D_k$ . In consequence, for two Gaussian distributions  $q_{g_k}(\mathbf{x}'|\mathbf{z}, \boldsymbol{\sigma}_k)$  and  $p(\mathbf{z})$ , the KL-divergence can be expressed analytically:

$$D_{KL}(q_{g_k}(\mathbf{x}'|\mathbf{z}, \boldsymbol{\sigma}_k)||p(\mathbf{z})) = \frac{1}{2} \{(\mathbf{z} - \mathbf{c}^y)^T(\mathbf{z} - \mathbf{c}^y) + \text{tr}(\Sigma_k) - p - \log|\Sigma_k|\} \quad (3)$$

Therefore, we design a negative ELBO loss  $\mathcal{L}_e$  to optimize  $g_k$ ,  $\psi_k$  and  $\boldsymbol{\sigma}_k$ :

$$\begin{aligned} \mathcal{L}_e &= \sum_{y \in \mathcal{Y}_k} \frac{1}{|D_k^y|} \sum_{i=1}^{|D_k^y|} \mathcal{L}_{rc}(\mathbf{x}'_i, \mathbf{x}_i) + D_{KL}(q_{g_k}(\mathbf{z}_i|\mathbf{x}_i)||p(\mathbf{z})) \\ &= \sum_{y \in \mathcal{Y}_k} \frac{1}{|D_k^y|} \sum_{i=1}^{|D_k^y|} \|\mathbf{x}'_i - \mathbf{x}_i\|_2^2 + \frac{1}{2} \{(\mathbf{z}_i - \mathbf{c}^y)^T(\mathbf{z}_i - \mathbf{c}^y) + \text{tr}(\Sigma_k) - p - \log|\Sigma_k|\} \end{aligned} \quad (4)$$

$\mathcal{Y}_k = \{y : D_k^y \neq \emptyset, 1 \leq y \leq C\}$  indicates all possible classes from client  $k$ 's data.

As Figure 2 shows, to mitigate the bias of the local distribution  $\mathcal{N}(\mathbf{z}, \Sigma_k)$ , each client  $k$  will update the local class-wise prototypes  $\{\mathbf{c}_k^y\}_{y \in \mathcal{Y}_k}$  and the SD  $\boldsymbol{\sigma}_k$  to the server. In response, the server obtains the global prototypes  $\{\mathbf{c}^y\}$  and SD  $\boldsymbol{\sigma}$  through aggregation, and sends  $\{\mathbf{c}^y\}, \boldsymbol{\sigma}$  back to clients.

### 3.3 Regularizing VTC for Better Generalization

Owing to the randomness of the TC process,  $\psi_k$  is likely to generate variant synthetic samples  $\{\mathbf{x}'\}$  with unknown training quality. To address this issue, we propose to regularize the training procedure of VTC with a distribution matching (DM) loss  $\mathcal{L}_{dm}$ :

$$\mathcal{L}_{dm} = \sum_{y \in \mathcal{Y}_k} \frac{1}{|D_k^y|} \sum_{i=1}^{|D_k^y|} \|g_k(\mathbf{x}'_i) - \mathbf{c}^y\|_2^2 = \sum_{y \in \mathcal{Y}_k} \frac{1}{|D_k^y|} \sum_{i=1}^{|D_k^y|} \|g_k(\psi_k(\mathbf{v}_i)) - \mathbf{c}^y\|_2^2 \quad (5)$$

This loss enforces  $\psi_k$  to generate high-quality samples in which  $g_k$  can acquire a feature distribution close to the unbiased global distribution [39]. Subsequently, the local model  $f_k$  will learn unbiased parameter updates from the synthetic data, resulting in better generalization performance.

Overall, the loss function  $\mathcal{L}_{tc}$  to train a VTC model is defined as:

$$\mathcal{L}_{tc} = \mathcal{L}_e + \lambda \mathcal{L}_{dm} \quad (6)$$

$\lambda > 0$  is the coefficient of regularization.

---

**Algorithm 1** FedVTC

---

**Require:** FL iterations  $T$ , fine-tuning rounds  $\mathcal{T}$ , local epochs  $E$ , clients  $\mathcal{K} = \{1, \dots, K\}$ , local models  $\{f_1, \dots, f_K\}$ , datasets  $\{D_1, \dots, D_K\}$ , local TCs  $\{\psi_1, \dots, \psi_K\}$ , local SDs  $\{\sigma_1, \dots, \sigma_K\}$ , initial SD  $\sigma$ , initial prototypes  $\{c^1, \dots, c^C\}$  learning rate  $\eta$ , number of generated samples  $S$ .

- 1: **for**  $t = 1, 2, \dots, T$  **do**
- 2:     **server does:**
- 3:         randomly sample a set of participating clients  $\mathcal{K}^t \subset \mathcal{K}$ .
- 4:         **for**  $y \in \{1, \dots, C\}$ :
- 5:              $\mathcal{K}_y^t \leftarrow \mathcal{K}^t \cap \mathcal{K}_y$ .
- 6:             broadcast  $c^y$  to clients in  $\mathcal{K}_y^t$ .
- 7:             broadcast  $\sigma$  to clients in  $\mathcal{K}^t$ .
- 8:         **every client**  $k \in \mathcal{K}^t$  **does:**
- 9:              $\sigma_k \leftarrow \sigma$ .
- 10:            **for** epochs  $1, \dots, E$ :
- 11:                $f_k \leftarrow f_k - \eta \nabla_{f_k} \mathcal{L}$ . ▷ Update  $f_k$  with SGD.
- 12:                $g_k \leftarrow g_k - \eta \nabla_{g_k} \mathcal{L}_{tc}$ ,  $\psi_k \leftarrow \psi_k - \eta \nabla_{\psi_k} \mathcal{L}_{tc}$ ,  $\sigma_k \leftarrow \sigma_k - \eta \nabla_{\sigma_k} \mathcal{L}_{tc}$ .
- 13:               **for**  $y \in \mathcal{Y}_k$ :
- 14:                    $c_k^y \leftarrow \frac{1}{|D_k^y|} \sum_{\mathbf{x} \in D_k^y} g_k(\mathbf{x})$ . ▷ Compute local prototype.
- 15:                   upload  $c_k^y$  to the server.
- 16:                   upload  $\sigma_k$  to the server.
- 17:            **server does:**
- 18:               **for**  $y \in \{1, \dots, C\}$ :
- 19:                    $c^y \leftarrow \frac{1}{|\mathcal{K}_y^t|} \sum_{k \in \mathcal{K}_y^t} c_k^y$ . ▷ Update global prototype.
- 20:                    $\sigma \leftarrow \frac{1}{|\mathcal{K}^t|} \sum_{k \in \mathcal{K}^t} \sigma_k$ . ▷ Update global SD.
- 21:            **end for**
- 22:         **every client**  $k \in \mathcal{K}$  **does:**
- 23:             upload  $\psi_k$  to the server.
- 24:         **server does:**
- 25:              $\psi \leftarrow \frac{1}{K} \sum_{k=1}^K \psi_k$ . ▷ obtain global TC.
- 26:             broadcast  $\psi, \{c^1, \dots, c^C\}$  and  $\sigma$  to every client  $k \in \mathcal{K}$ .
- 27:         **for** every  $k \in \mathcal{K}$  **do**
- 28:             create synthetic dataset  $D'_k$  with  $S$  samples using  $\psi, \sigma$  and  $\{c^1, \dots, c^C\}$ .
- 29:             **for** rounds  $1, \dots, \mathcal{T}$ :
- 30:                  $\mathcal{L}' \leftarrow \frac{1}{S} \sum_{i=1}^S (y'_i, f(\mathbf{x}'_i))$ .
- 31:                  $f_k \leftarrow f_k - \eta \nabla_{f_k} \mathcal{L}'$ . ▷ fine-tuning with the synthetic dataset.
- 32:             **end for**
- 33:         **return**  $w^t$

---

### 3.4 FedVTC Overview

The comprehensive FedVTC framework is presented in Algorithm 1. Specifically, for each iteration  $t$ , every active client  $k$  regularly trains the local model  $f_k$  as in traditional FL. In addition,  $k$  trains  $\psi_k$  and  $\sigma_k$  using loss function  $\mathcal{L}_{tc}$  (Equation 6). Afterwards,  $k$  uploads the local prototypes and SD to the server for aggregation. The server averages the received results and returns the global prototype and SD to clients.

For memory efficiency, FedVTC applies an alternating strategy in VTC training. For line 12 in Algorithm 1, we first freeze  $\psi_k$  and  $\sigma_k$  and incorporate the step  $g_k \leftarrow g_k - \eta \nabla_{g_k} \mathcal{L}_{tc}$  into the standard training of  $f_k$ . In this case, line 11 in Algorithm 1 can be written as  $f_k \leftarrow f_k - \eta \nabla_{f_k} (\mathcal{L} + \mathcal{L}_{tc})$  (with  $g_k$  included in  $f_k$ ). Then we freeze  $f_k$  and optimize  $\psi_k$  and  $\sigma_k$  with  $\mathcal{L}_{tc}$ . As a result, FedVTC will not extend the maximum memory usage, as  $\psi_k$  and  $\sigma_k$  usually require less memory space than  $f_k$  for training. In contrast, if we optimize  $f_k, \psi_k$  and  $\sigma_k$  simultaneously, the maximum memory usage will be enlarged to their accumulated memory usage.

Once FL is complete, every client  $k \in \mathcal{K}$  uploads the local TC  $\psi_k$  to the server, then the server derives a global TC  $\psi$  through aggregation, and broadcasts  $\psi$  along with  $\{c^1, \dots, c^C\}, \sigma$  to all clients. In order to aggregate TC parameters, FedVTC lets all  $\psi_k$ 's have the same architecture. For

each  $c^y$  ( $y \in \{1, \dots, C\}$ ), every client  $k$  samples  $\frac{S}{C}$  latent variables from distribution  $\mathcal{N}(c^y, \Sigma)$ , and generates the corresponding synthetic samples by forwarding these variables to  $\psi$ .  $\Sigma \in \mathbb{R}^{p \times p}$  is a diagonal matrix with  $\Sigma_{ii}$  equal to the squared  $i$ -th element in  $\sigma$ . Afterwards, each client fine-tunes its local model by running classification tasks on the total  $S$  synthetic samples. In this stage, all local fine-tuning processes run in isolation, and no communication occurs between clients and the server.

One noteworthy point in FedVTC is that, clients only need to upload the local TC models once instead of every FL iteration (see line 23 in Algorithm 1). In the experiment, we compare the performance of FedVTC in cases of singular TC transmission and per-round TC transmission. The results show that these two modules exhibit marginal differences in terms of accuracy (see Table 3). Therefore, in the ultimate FedVTC framework, local TCs are only communicated once for communication efficiency.

## 4 Experiments

### 4.1 Experiment Setup

**Datasets.** We evaluate FedVTC on the following datasets: MNIST [41] contains a training set with 60,000 samples and a validation set with 10,000 samples from 10 classes. CIFAR10 and CIFAR100 [42] contain a training set with 50,000 samples and a validation set of 10,000 samples from 10 and 100 classes. Tiny-ImageNet [43] contains a training set with 100,000 samples and a validation set with 10,000 samples from 200 classes.

**Comparative methods.** We compare FedVTC with five state-of-the-art model-heterogeneous FL frameworks. **1. FedProto** [35] enables clients to regularize the local feature extractors using class-wise global prototypes. **2. FedTGP** [36] extends the design of FedProto by optimizing the decision boundary between inter-class prototypes using gradient descent. **3. FedGen** [33] and **4. CCVR** [34] utilize virtual feature representations to fine-tune the classifiers of clients, with FedGen using a generative adversarial network (GAN) and CCVR using a Gaussian distribution to generate the representations. **5. FedType** [37] allows clients to collaboratively train a proxy model using conformal prediction and enhance generalization by distilling knowledge through the proxy model.

**System implementation.** We simulate a virtual network consisting of  $K = 100$  clients with a participation rate of 0.1 (i.e.  $|\mathcal{K}^t| = 10$ ). Both the server and all clients operate on one NVIDIA Geforce RTX 4070 GPU with 12 GB of RAM space. For heterogeneous client models, we follow the settings in [36, 37], where clients are divided into five uniform clusters with five model architectures: ResNet-18, ResNet-34, ResNet-50, ResNet-101 and ResNet-152 [44]. For non-iid local data distribution, we follow [34] and distribute the training sets of MNIST, CIFAR10, CIFAR100, and Tiny-ImageNet unevenly among clients using two Dirichlet (*Dir*) distributions with parameters 0.1 and 1.0. The experiment platform is implemented with PyTorch 2.0 [45]. The TC model has a simple architecture with four layers (see Appendix B.3).

**Parameter settings.** Following [35, 37], the total number of iterations is set to  $T = 100$ . For FedVTC, the number of additional fine-tuning rounds is set to  $\mathcal{T} = 5$ . For fairness, we also let the baselines train extra  $\mathcal{T}$  rounds with full client participation so that all methods have the same training rounds. The learning rate  $\eta$  is set to  $1e-4$  for MNIST [34] and  $0.01$  for others [35]. The local epoch  $E$  is set to five, and the batch size is set to 16 universally [37]. For fairness, the number of synthetic samples  $S$  is set to 500 for MNIST and CIFAR10, and 1000 for CIFAR100 and Tiny-ImageNet, which is identical to the amount of generated representations in [34]. Lastly, we set the regularization parameter as  $\lambda = 0.1$  following [36]. The settings of  $p$  and  $d$  can be found in Appendix B.1.

### 4.2 Experiment Results

**Generalization accuracy.** We use the validation sets in the aforementioned four datasets to evaluate the average generalization accuracy of each client. Each method runs for three independent trials, and the average results are recorded. As shown in Table 1, FedVTC consistently outperforms the comparative methods across all datasets and distributions, demonstrating a remarkable generalization ability over non-iid data. As a supplementary, the graphs depicting accuracy per iteration are included in Appendix B.2.

**Communication efficiency.** As shown in Table 2, FedVTC obtains the least overall communication cost among all methods. Specifically, for CCVR, clients share the local prototypes and covariates with

		FedProto	FedTGP	FedGen	CCVR	FedType	<b>FedVTC</b>
MNIST	<i>Dir</i> (0.1)	83.4±0.4	85.4±0.5	81.1±1.0	85.5±0.4	83.9±0.3	<b>88.7±0.7</b>
	<i>Dir</i> (1.0)	86.1±0.3	86.8±0.4	81.9±0.3	86.2±0.3	86.7±0.5	<b>90.1±0.1</b>
CIFAR10	<i>Dir</i> (0.1)	39.3±0.7	40.9±0.2	39.1±0.2	39.3±0.2	39.7±0.3	<b>46.9±0.6</b>
	<i>Dir</i> (1.0)	41.1±0.2	42.1±0.7	39.7±0.5	41.0±0.1	40.2±0.6	<b>51.7±0.7</b>
CIFAR100	<i>Dir</i> (0.1)	26.2±0.2	29.2±0.3	27.3±0.8	27.6±0.9	31.3±1.5	<b>36.3±0.8</b>
	<i>Dir</i> (1.0)	30.4±0.2	31.8±0.5	30.8±0.3	29.3±0.4	34.4±0.6	<b>40.4±0.3</b>
Tiny-ImageNet	<i>Dir</i> (0.1)	23.7±0.3	24.9±0.8	23.6±0.1	24.1±0.3	24.8±0.4	<b>30.2±0.3</b>
	<i>Dir</i> (1.0)	26.4±0.2	27.2±0.3	26.1±0.1	26.6±0.8	31.6±0.4	<b>35.8±0.5</b>

Table 1: The average generalization accuracy (in %) of each local model on the public validation dataset (with mean  $\pm$  SD).

	FedProto	FedTGP	FedGen	CCVR	FedType	<b>FedVTC</b>
MNIST	0.94	0.94	13.15	46.61	12.37	<b>0.70</b>
CIFAR10	3.93	3.93	54.58	807.46	37.45	<b>2.90</b>
CIFAR100	39.32	39.32	91.07	825.16	72.85	<b>26.49</b>
Tiny-ImageNet	78.64	78.64	844.82	923.46	179.61	<b>52.71</b>

Table 2: The total volume of data transmission (in GB).

the server. Although transmitting the  $p$ -dimensional prototypes introduces marginal communication cost, this cost grows exponentially for transmitting the covariance matrices of a  $p \times p$  dimension. For FedGen and FedType, the server respectively broadcasts a generator (2-layer perception [33]) and a proxy model (ResNet-18 [37]) to clients, while these overparametrized models usually consume massive communication resources in transmission. In comparison, FedProto and FedTGP only transmit prototypes with significantly less communication costs. Although FedVTC transmits additional messages other than prototypes, including SDs and TC models, it still reduces the total communication costs compared with FedProto and FedTGP, as no information is transmitted in the phase of fine-tuning.

**Memory requirement.** We calculate the required memory space of each method by accumulating the magnitudes of parameter weights, gradients and activations involved in training according to [46]. As depicted in Figure 3, compared with other methods, FedVTC accounts for an equivalent or less memory space across all model architectures. We attribute this to the strategy of alternately training local models and TC models in FedVTC. In contrast, FedType, which simultaneously trains local models and the proxy model, demands a much higher memory space for training.

**Ablation study.** We compare the performance of FedVTC with two modules of TC transmission, including **singular** (TC models are communicated only once) and **regular** (TC models are communicated every round) transmissions. As shown in Table 3, the generalization accuracy of singular TC transmission is slightly lower (sometimes even higher) than regular TC transmission, while the latter causes much higher communication cost than the former. Therefore, we apply the singular TC transmission strategy in the ultimate FedVTC framework for communication efficiency. Fur-

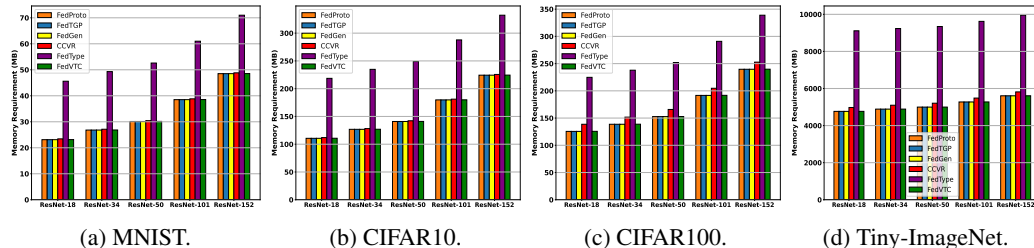


Figure 3: FedVTC (green) has an equivalent or less memory requirement compared with others.

		MNIST		CIFAR10		CIFAR100		Tiny-ImageNet	
		<i>Dir</i> (0.1)	<i>Dir</i> (1.0)						
*	①	88.7(0.7)	90.1(0.1)	<b>46.9</b> (0.6)	51.7(0.7)	36.3(0.8)	<b>40.4</b> (0.3)	30.2(0.3)	35.8(0.5)
	②	<b>89.7</b> (0.2)	<b>92.3</b> (0.3)	45.4(0.3)	<b>54.3</b> (0.5)	<b>37.7</b> (0.4)	39.6(0.6)	<b>31.8</b> (0.7)	<b>38.0</b> (1.0)
**	①	<b>0.70</b>		<b>2.90</b>		<b>26.49</b>		<b>52.71</b>	
	②	5.63		8.77		32.36		123.22	

Table 3: The (\*)generalization accuracy (%) and (\*\*)communication cost (GB) of ①FedVTC with singular TC transmission and ②FedVTC with regular TC transmission per round.

	MNIST		CIFAR10		CIFAR100		Tiny-ImageNet	
	<i>Dir</i> (0.1)	<i>Dir</i> (1.0)						
$\mathcal{L}_e$	87.2(0.4)	89.9(0.3)	39.7(0.5)	45.4(0.4)	28.9(0.5)	35.2(0.2)	28.1(0.1)	33.4(0.3)
$\mathcal{L}_{tc}$	<b>88.7</b> (0.7)	<b>90.1</b> (0.1)	<b>46.9</b> (0.6)	<b>51.7</b> (0.7)	<b>36.3</b> (0.8)	<b>40.4</b> (0.3)	<b>30.2</b> (0.3)	<b>35.8</b> (0.5)

Table 4: The generalization accuracy of two training modules of FedVTC. The first module uses the standard  $\mathcal{L}_e$  loss, and the second module uses the regularized  $\mathcal{L}_{tc} = \mathcal{L}_e + \lambda\mathcal{L}_{dm}$  loss.



Figure 4: A fraction of raw images (top) and synthetic images (bottom) on MNIST and CIFAR10.

thermore, we compare two training modules of FedVTC, where the VTC is trained with  $\mathcal{L}_e$  and  $\mathcal{L}_{tc} = \mathcal{L}_e + \lambda\mathcal{L}_{dm}$  respectively. As shown in Table 4, the DM-based regularization effectively increases the generalization performance of FedVTC in all scenarios.

**Privacy preservation.** FedVTC transmits prototypes, SDs and TC models, which brings no additional privacy concerns according to [34, 35]. The reason is that, it is almost impossible to recover the raw data from prototypes and SDs without accessing the raw representations. As Figure 4 shows, the VTC-generated images diverge drastically from real images, making it extremely difficult to capture any sensitive information from these images.

## 5 Conclusion

This paper proposes FedVTC, a model-heterogeneous FL framework based on variational transposed convolution (VTC). By fine-tuning local models with VTC-generated samples, FedVTC effectively overcomes the low-generalization bottleneck of FL clients in model-heterogeneous settings without relying on any public datasets. Furthermore, we regularize the VTC training procedure with a distribution matching loss, further improving the quality of the synthetic samples and leading to higher generalization accuracy. Lastly, FedVTC maintains communication and memory efficiency due to the lightweight distribution transmission and alternating training strategy.

**Broader impact.** We expect FedVTC to promote the application of generative models to address the data shortage problem in the FL community. From the generated data with high training quality and unrealistic context, clients can acquire sufficient knowledge of the global distribution without violating data privacy. This property is crucial to help FL clients maintain performance with insufficient training data. Moreover, abstaining from parameter transmission, FedVTC significantly alleviates the risk of model-based malicious attacks, such as Byzantine attacks [17] and model inversion attacks [47].

**Limitations and future works.** The main limitation of FedVTC is the additional computation overhead of training a VTC model. As a remedy, we can consolidate FedVTC with the early-stopping technique [23] to mitigate the overall computation cost. In addition, we plan to amplify the adaptability of FedVTC to data from unseen classes with techniques like zero-shot learning [48] and model diffusion [49].

## References

- [1] B. McMahan, E. Moore, D. Ramage, S. Hampson, and B. A. y. Arcas, “Communication-efficient learning of deep networks from decentralized data,” in *Artificial Intelligence and Statistics*, 2017, pp. 1273–1282.
- [2] P. Abeyssekara, H. Dong, and A. K. Qin, “Data-driven trust prediction in mobile edge computing-based iot systems,” *IEEE Transactions on Services Computing*, vol. 16, no. 1, pp. 246–260, 2023.
- [3] C. Mclaughlin and L. Su, “Personalized federated learning via feature distribution adaptation,” *Proceedings of the 38th Conference on Neural Information Processing Systems (NeurIPS 2024)*, vol. 37, pp. 77 038–77 059, 2024.
- [4] N. P. Reddy, S. K. Hassain, P. Baraneedharan, and S. A. Rahman, “Internet of things-based remote weather forecasting system using legacy sensors,” in *Proceedings of the 9th International Conference on Advanced Computing and Communication Systems (ICACCS 2023)*, vol. 1, 2023, pp. 2305–2309.
- [5] H. N. Saha, S. Auddy, S. Pal, S. Kumar, S. Pandey, R. Singh, A. K. Singh, P. Sharan, D. Ghosh, and S. Saha, “Health monitoring using internet of things (iot),” in *Proceedings of the 8th Annual Industrial Automation and Electromechanical Engineering Conference (IEMECON 2017)*, 2017, pp. 69–73.
- [6] Z. Sun, X. Niu, and E. Wei, “Understanding generalization of federated learning via stability: Heterogeneity matters,” in *Proceedings of The 27th International Conference on Artificial Intelligence and Statistics (AISTATS)*, vol. 238, 2024, pp. 676–684.
- [7] C.-Y. Huang, K. Srinivas, X. Zhang, and X. Li, “Overcoming data and model heterogeneities in decentralized federated learning via synthetic anchors,” *arXiv preprint arXiv:2405.11525*, 2024.
- [8] C. T. Dinh, N. H. Tran, and T. D. Nguyen, “Personalized federated learning with moreau envelopes,” in *Proceedings of the 34th Conference on Neural Information Processing Systems (NeurIPS 2020)*, 2020.
- [9] T. Li, S. Hu, A. Beirami, and V. Smith, “Ditto: Fair and robust federated learning through personalization,” in *Proceedings of the 2021 International Conference on Machine Learning (ICML 2021)*, 2021, pp. 6357–6368.
- [10] T. Li, A. K. Sahu, M. Zaheer, M. Sanjabi, A. Talwalkar, and V. Smith, “Federated optimization in heterogeneous networks,” *Proceedings of the 2020 Conference on Machine Learning and Systems (MLSys 2020)*, pp. 429–450, 2020.
- [11] V. Smith, C.-K. Chiang, M. Sanjabi, and A. S. Talwalkar, “Federated multi-task learning,” *Proceedings of the 31st Conference on Neural Information Processing Systems (NIPS 2017)*, vol. 30, 2017.
- [12] S. P. Karimireddy, S. Kale, M. Mohri, S. Reddi, S. Stich, and A. T. Suresh, “SCAFFOLD: Stochastic controlled averaging for federated learning,” in *Proceedings of the 37th International Conference on Machine Learning (ICML 2020)*, vol. 119, 2020, pp. 5132–5143.
- [13] D. A. E. Acar, Y. Zhao, R. Matas, M. Mattina, P. Whatmough, and V. Saligrama, “Federated learning based on dynamic regularization,” in *Proceedings of the 2021 International Conference on Learning Representations (ICLR 2021)*, 2021.
- [14] L. Gao, H. Fu, L. Li, Y. Chen, M. Xu, and C.-Z. Xu, “Feddc: Federated learning with non-iid data via local drift decoupling and correction,” in *Proceedings of the 2022 IEEE/CVF Conference on Computer Vision and Pattern Recognition (CVPR 2022)*, June 2022, pp. 10 112–10 121.
- [15] X. Li, K. Huang, W. Yang, S. Wang, and Z. Zhang, “On the convergence of fedavg on non-iid data,” *arXiv preprint arXiv:1907.02189*, 2019.
- [16] K. Pillutla, S. M. Kakade, and Z. Harchaoui, “Robust aggregation for federated learning,” *IEEE Transactions on Signal Processing*, vol. 70, pp. 1142–1154, 2022.
- [17] X. Cao, M. Fang, J. Liu, and N. Z. Gong, “Fltrust: Byzantine-robust federated learning via trust bootstrapping,” *arXiv preprint arXiv:2012.13995*, 2020.
- [18] X. Mu, K. Cheng, Y. Shen, X. Li, Z. Chang, T. Zhang, and X. Ma, “Feddmc: Efficient and robust federated learning via detecting malicious clients,” *IEEE Transactions on Dependable and Secure Computing*, vol. 21, no. 6, pp. 5259–5274, 2024.

- [19] S. Li, Y. Cheng, W. Wang, Y. Liu, and T. Chen, “Learning to detect malicious clients for robust federated learning,” *arXiv preprint arXiv:2002.00211*, 2020.
- [20] F. Tahmasebian, J. Lou, and L. Xiong, “Robustfed: A truth inference approach for robust federated learning,” in *Proceedings of the 2022 International Conference on Information and Knowledge Management (CIKM 2022)*, 2022, p. 1868–1877.
- [21] Y. Jee Cho, J. Wang, and G. Joshi, “Towards understanding biased client selection in federated learning,” in *Proceedings of the 25th International Conference on Artificial Intelligence and Statistics (AISTATS 2022)*, vol. 151, 2022, pp. 10 351–10 375.
- [22] C. Li, X. Zeng, M. Zhang, and Z. Cao, “Pyramidfl: A fine-grained client selection framework for efficient federated learning,” in *Proceedings of the 28th Annual International Conference on Mobile Computing and Networking (MobiCom 2022)*, 2022, p. 158–171.
- [23] Z. Niu, H. Dong, A. K. Qin, and T. Gu, “Flrce: Resource-efficient federated learning with early-stopping strategy,” *IEEE Transactions on Mobile Computing*, vol. 23, no. 12, pp. 14 514–14 529, 2024.
- [24] J. Zhang, A. Li, M. Tang, J. Sun, X. Chen, F. Zhang, C. Chen, Y. Chen, and H. Li, “Fed-CBS: A heterogeneity-aware client sampling mechanism for federated learning via class-imbalance reduction,” in *Proceedings of the 40th International Conference on Machine Learning (ICML 2023)*, vol. 202, 2023, pp. 41 354–41 381.
- [25] F. Lai, X. Zhu, H. V. Madhyastha, and M. Chowdhury, “Oort: Efficient federated learning via guided participant selection,” in *Proceedings of the 15th USENIX Symposium on Operating Systems Design and Implementation (OSDI 2021)*, 2021, pp. 19–35.
- [26] D. Li and J. Wang, “Fedmd: Heterogenous federated learning via model distillation,” *arXiv preprint arXiv:1910.03581*, 2019.
- [27] S. Itahara, T. Nishio, Y. Koda, M. Morikura, and K. Yamamoto, “Distillation-based semi-supervised federated learning for communication-efficient collaborative training with non-iid private data,” *IEEE Transactions on Mobile Computing*, vol. 22, no. 1, pp. 191–205, 2023.
- [28] Y. J. Cho, A. Manoel, G. Joshi, R. Sim, and D. Dimitriadis, “Heterogeneous ensemble knowledge transfer for training large models in federated learning,” in *Proceedings of the Thirty-First International Joint Conference on Artificial Intelligence (IJCAI-22)*, 7 2022, pp. 2881–2887, main Track.
- [29] D. P. Nguyen, S. Yu, J. P. Muñoz, and A. Jannesari, “Enhancing heterogeneous federated learning with knowledge extraction and multi-model fusion,” in *Proceedings of the SC '23 Workshops of the International Conference on High Performance Computing, Network, Storage, and Analysis (SC-W 2023)*, New York, NY, USA, 2023, p. 36–43.
- [30] S. Cheng, J. Wu, Y. Xiao, Y. Liu, and Y. Liu, “Fedgems: Federated learning of larger server models via selective knowledge fusion,” *arXiv preprint arXiv:2110.11027*, 2021.
- [31] L. Sun and L. Lyu, “Federated model distillation with noise-free differential privacy,” in *Proceedings of the Thirtieth International Joint Conference on Artificial Intelligence (IJCAI-21)*, 2021, pp. 1563–1569.
- [32] F. Sattler, T. Korjakow, R. Rischke, and W. Samek, “Fedaux: Leveraging unlabeled auxiliary data in federated learning,” *IEEE Transactions on Neural Networks and Learning Systems*, vol. 34, no. 9, pp. 5531–5543, 2021.
- [33] Z. Zhu, J. Hong, and J. Zhou, “Data-free knowledge distillation for heterogeneous federated learning,” in *Proceedings of the 2021 International Conference on Machine Learning (ICML 2021)*, 2021, pp. 12 878–12 889.
- [34] M. Luo, F. Chen, D. Hu, Y. Zhang, J. Liang, and J. Feng, “No fear of heterogeneity: Classifier calibration for federated learning with non-IID data,” in *Proceedings of the 35th Conference on Neural Information Processing Systems (NeurIPS 2021)*, 2021.
- [35] Y. Tan, G. Long, L. Liu, T. Zhou, Q. Lu, J. Jiang, and C. Zhang, “Fedproto: Federated prototype learning across heterogeneous clients,” in *Proceedings of the 2022 AAAI Conference on Artificial Intelligence (AAAI 2022)*, vol. 36, 2022, pp. 8432–8440.
- [36] J. Zhang, Y. Liu, Y. Hua, and J. Cao, “Fedtgp: Trainable global prototypes with adaptive-margin-enhanced contrastive learning for data and model heterogeneity in federated learning,”

- in *Proceedings of the 2024 AAAI Conference on Artificial Intelligence (AAAI 2024)*, vol. 38, no. 15, 2024, pp. 16 768–16 776.
- [37] J. Wang, C. Zhao, L. Lyu, Q. You, M. Huai, and F. Ma, “Bridging model heterogeneity in federated learning via uncertainty-based asymmetrical reciprocity learning,” in *Proceedings of the 41st International Conference on Machine Learning (ICML 2024)*, 2024.
- [38] D. P. Kingma and M. Welling, “Auto-encoding variational bayes,” *arXiv preprint arXiv:1312.6114*, 2013.
- [39] G. Zhao, G. Li, Y. Qin, and Y. Yu, “Improved distribution matching for dataset condensation,” in *Proceedings of the 2023 IEEE/CVF Conference on Computer Vision and Pattern Recognition (CVPR 2023)*, 2023, pp. 7856–7865.
- [40] V. Dumoulin and F. Visin, “A guide to convolution arithmetic for deep learning,” *arXiv preprint arXiv:1603.07285*, 2016.
- [41] Y. LeCun. (1998). [Online]. Available: <http://yann.lecun.com/exdb/mnist/>
- [42] A. Krizhevsky, “Learning multiple layers of features from tiny images,” *University of Toronto*, 2009.
- [43] P. Chrabaszcz, I. Loshchilov, and F. Hutter, “A downsampled variant of imagenet as an alternative to the cifar datasets,” *arXiv preprint arXiv:1707.08819*, 2017.
- [44] K. He, X. Zhang, S. Ren, and J. Sun, “Deep residual learning for image recognition,” in *Proceedings of the 2016 IEEE Conference on Computer Vision and Pattern Recognition (CVPR 2016)*, 2016, pp. 770–778.
- [45] A. Paszke, S. Gross, F. Massa, A. Lerer, J. Bradbury, G. Chanan, T. Killeen, Z. Lin, N. Gimelshein, L. Antiga, A. Desmaison, A. Köpf, E. Yang, Z. DeVito, M. Raison, A. Tejani, S. Chilamkurthy, B. Steiner, L. Fang, J. Bai, and S. Chintala, *PyTorch: an imperative style, high-performance deep learning library*. Curran Associates Inc., 2019, vol. 32, pp. 8024–8035.
- [46] K. Pfeiffer, R. Khalili, and J. Henkel, “Aggregating capacity in FL through successive layer training for computationally-constrained devices,” in *Proceedings of the 37th Conference on Neural Information Processing Systems (NeurIPS 2023)*, 2023.
- [47] N.-B. Nguyen, K. Chandrasegaran, M. Abdollahzadeh, and N.-M. Cheung, “Re-thinking model inversion attacks against deep neural networks,” in *Proceedings of the 2023 IEEE/CVF Conference on Computer Vision and Pattern Recognition (CVPR 2023)*, 2023, pp. 16 384–16 393.
- [48] X. Chen, X. Deng, Y. Lan, Y. Long, J. Weng, Z. Liu, and Q. Tian, “Explanatory object part aggregation for zero-shot learning,” *IEEE Transactions on Pattern Analysis and Machine Intelligence*, vol. 46, no. 2, pp. 851–868, 2024.
- [49] F.-A. Croitoru, V. Hondru, R. T. Ionescu, and M. Shah, “Diffusion models in vision: A survey,” *IEEE Transactions on Pattern Analysis and Machine Intelligence*, vol. 45, no. 9, pp. 10 850–10 869, 2023.
- [50] M. Ye, X. Fang, B. Du, P. C. Yuen, and D. Tao, “Heterogeneous federated learning: State-of-the-art and research challenges,” *ACM Computing Surveys*, vol. 56, no. 3, 2023.
- [51] S. Caldas, J. Konečný, H. B. McMahan, and A. Talwalkar, “Expanding the reach of federated learning by reducing client resource requirements,” in *NeurIPS Workshop on Federated Learning for Data Privacy and Confidentiality*, 2018.
- [52] S. Horváth, S. Laskaridis, M. Almeida, I. Leontiadis, S. Venieris, and N. Lane, “Fjord: Fair and accurate federated learning under heterogeneous targets with ordered dropout,” in *Proceedings of the 35th Conference on Neural Information Processing Systems (NeurIPS 2021)*, vol. 34, 2021, pp. 12 876–12 889.
- [53] E. Diao, J. Ding, and V. Tarokh, “Hetero{fl}: Computation and communication efficient federated learning for heterogeneous clients,” in *Proceedings of the 2021 International Conference on Learning Representations (ICLR 2021)*, 2021.
- [54] S. Alam, L. Liu, M. Yan, and M. Zhang, “Fedrolex: model-heterogeneous federated learning with rolling sub-model extraction,” in *Proceedings of 31st Conference on Neural Information Processing Systems (NeurIPS 2022)*, 2022.

- [55] Z. Jiang, Y. Xu, H. Xu, Z. Wang, J. Liu, Q. Chen, and C. Qiao, "Computation and communication efficient federated learning with adaptive model pruning," *IEEE Transactions on Mobile Computing*, pp. 1–18, 2023.
- [56] A. Li, J. Sun, P. Li, Y. Pu, H. Li, and Y. Chen, "Hermes: An efficient federated learning framework for heterogeneous mobile clients," in *Proceedings of the 27th Annual International Conference on Mobile Computing and Networking (MobiCom 2021)*, 2021, p. 420–437.
- [57] Y. Jiang, S. Wang, V. Valls, B. J. Ko, W.-H. Lee, K. K. Leung, and L. Tassiulas, "Model pruning enables efficient federated learning on edge devices," *IEEE Transactions on Neural Networks and Learning Systems*, 2022.
- [58] M. Kim, S. Yu, S. Kim, and S.-M. Moon, "DepthFL : Depthwise federated learning for heterogeneous clients," in *Proceedings of the Eleventh International Conference on Learning Representations (ICLR 2023)*, 2023.

## A Definition of Model Heterogeneity

To our best knowledge, the definitions of "model-heterogeneous federated learning" in the state-of-the-art can be divided into the following two categories.

### A.1 Sub-model-based Model Heterogeneity

Sub-model-based model heterogeneity, also named *partial* model heterogeneity [50], is developed based on the assumption that all local models are a subset of the global model. Specifically, the server preserves a global model and employs the typical dropout technique [51] to extract a fraction of the global model's parameters, i.e., a *sub-model*, and allocates the sub-models to clients. For example, [51] generates sub-models by randomly pruning neurons in the global model. [52] and [53] consistently extract the left-most neurons of the global model to form sub-models. [54] dynamically extracts sub-models using a sliding window across the neurons in the global model. [55, 56, 57] selectively prune the unimportant neurons in the global model with the least heuristic scores (like parameter norms). [58] vertically extracts sub-models by pruning the top layers in the global model.

In these works, although clients have different model architectures due to different dropout strategies, the parameters between clients are usually co-dependent, and can be aggregated using sub-model aggregation as shown in Figure 5.

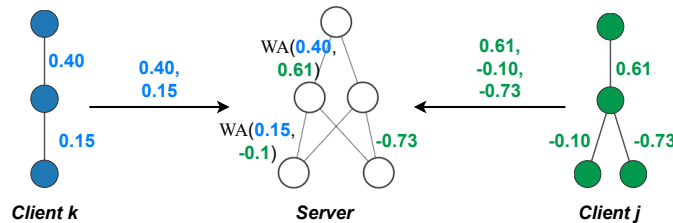


Figure 5: The sub-model aggregation scheme for sub-model-based model-heterogeneous FL ("WA" stands for weighted average).

### A.2 Complete Model Heterogeneity

In completely model-heterogeneous FL (shown in Figure 6), the server no longer maintains a global model, and clients obtain isolated local models with diverse, independent, and irrelevant architectures [50]. In this scenario, clients can no longer acquire generalized parameter updates through model aggregation. As a replacement, clients apply alternative strategies to learn generalization information, such as sharing knowledge over a public dataset or transmitting parameter-independent messages, as discussed in Section 2.2.

**Without ambiguity, in this paper, the definition of "model heterogeneity" refers to complete model heterogeneity (A.2) where all aggregation (e.g., standard aggregation and sub-model aggregation) methods become prohibitive. Correspondingly, the goal of FedVTC is to improve**

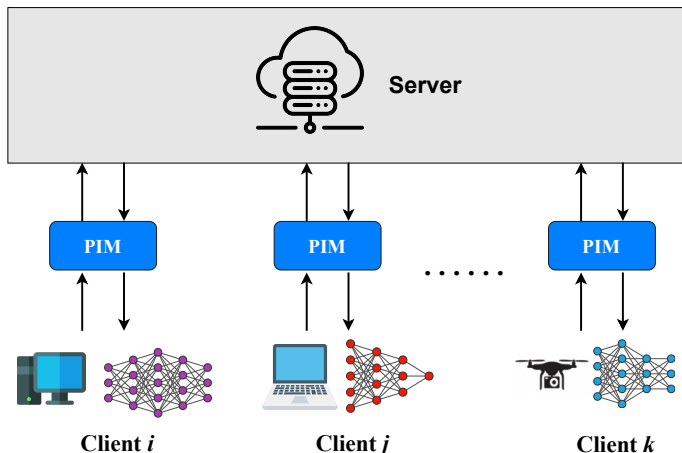


Figure 6: In complete model-heterogeneous FL, the model architectures between clients are independent, irrelevant, and cannot be aggregated altogether. Alternatively, clients communicate some Parameter-Independent Messages (PIM) with the server for knowledge sharing, such as prototypes and feature covariates.

**the generalization performance of clients in the settings of complete model heterogeneity without parameter aggregation involved.**

## B Experiment Details

	Channel	Input dimension $d$	Latent dimension $p$	Class $C$	Initial SD $\sigma$
MNIST	1	$1 \times 28 \times 28$	980	10	$\mathbf{1} \in \mathbb{R}^p$
CIFAR10	3	$3 \times 32 \times 32$	4096	10	
CIFAR100	3	$3 \times 32 \times 32$	4096	100	
Tiny-ImageNet	3	$3 \times 64 \times 64$	12768	200	

Table 5: Fundamental experimental settings.

### B.1 Fundamental Settings

The fundamental experimental settings are summarized in Table 5.

### B.2 Supplementary Results

The graphs reflecting the generalization accuracy against the FL iterations are shown in Figure 7.

### B.3 Structure of the Transposed Convolution Model

The detailed information on the structure of the TC model  $\psi$  is listed in Table 6.

MNIST			
Index	Components	Input shape	Output shape
1	TransposeConv2d(kernel=3, padding=1, stride=1) BatchNorm2d() LeakyReLU(0.01)	$20 \times 7 \times 7$	$16 \times 7 \times 7$
2	TransposeConv2d(kernel=4, padding=1, stride=2) BatchNorm2d() LeakyReLU(0.01)	$16 \times 7 \times 7$	$32 \times 14 \times 14$
3	TransposeConv2d(kernel=3, padding=1, stride=1) BatchNorm2d() LeakyReLU(0.01)	$32 \times 14 \times 14$	$32 \times 14 \times 14$
4	TransposeConv2d(kernel=4, padding=1, stride=2) BatchNorm2d() Sigmoid()	$32 \times 14 \times 14$	$1 \times 28 \times 28$

CIFAR10 & CIFAR100			
Index	Components	Input shape	Output shape
1	TransposeConv2d(kernel=3, padding=1, stride=1) BatchNorm2d() LeakyReLU(0.01)	$64 \times 8 \times 8$	$32 \times 8 \times 8$
2	TransposeConv2d(kernel=4, padding=1, stride=2) BatchNorm2d() LeakyReLU(0.01)	$32 \times 8 \times 8$	$64 \times 16 \times 16$
3	TransposeConv2d(kernel=3, padding=1, stride=1) BatchNorm2d() LeakyReLU(0.01)	$64 \times 16 \times 16$	$64 \times 16 \times 16$
4	TransposeConv2d(kernel=4, padding=1, stride=2) BatchNorm2d() Sigmoid()	$64 \times 16 \times 16$	$3 \times 32 \times 32$

Tiny-ImageNet			
Index	Components	Input shape	Output shape
1	TransposeConv2d(kernel=3, padding=1, stride=1) BatchNorm2d() LeakyReLU(0.01)	$128 \times 16 \times 16$	$64 \times 16 \times 16$
2	TransposeConv2d(kernel=4, padding=1, stride=2) BatchNorm2d() LeakyReLU(0.01)	$64 \times 16 \times 16$	$64 \times 32 \times 32$
3	TransposeConv2d(kernel=3, padding=1, stride=1) BatchNorm2d() LeakyReLU(0.01)	$64 \times 32 \times 32$	$64 \times 32 \times 32$
4	TransposeConv2d(kernel=4, padding=1, stride=2) BatchNorm2d() Sigmoid()	$64 \times 32 \times 32$	$3 \times 64 \times 64$

Table 6: Structural information on the transposed convolutional neural network.

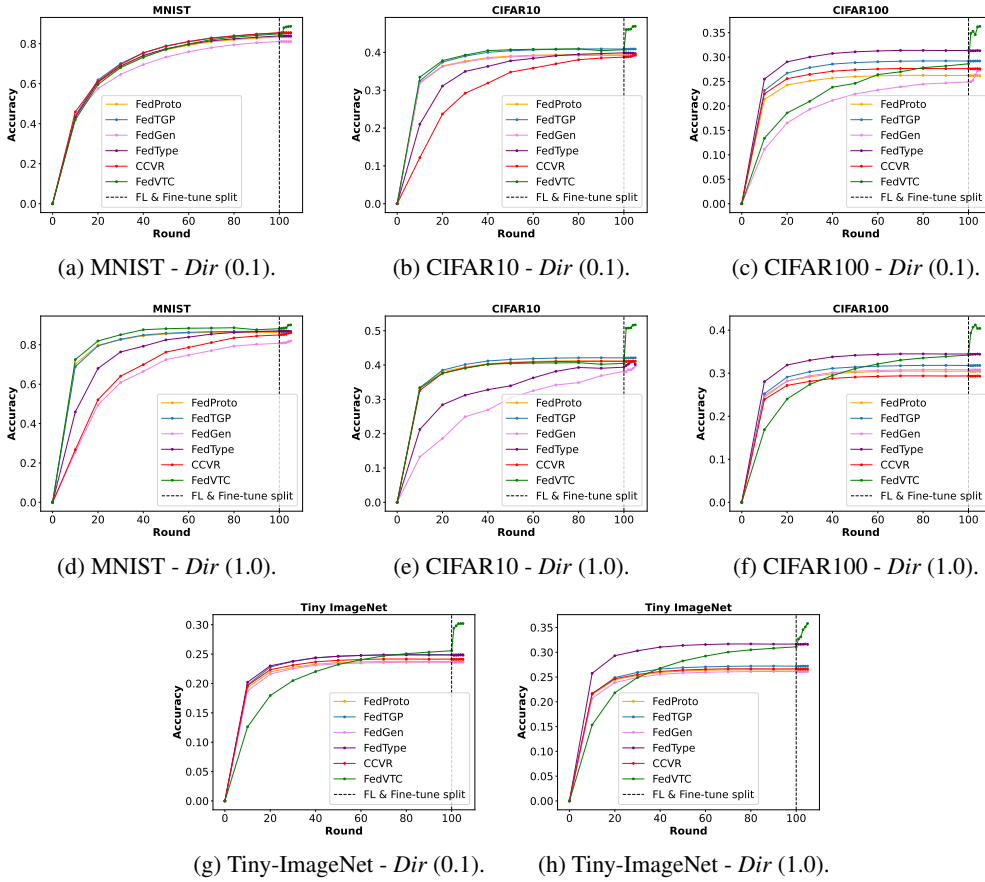


Figure 7: The graph of generalization accuracy per round. The vertical dashed line splits the standard FL iterations and the local fine-tuning procedure.